STEADY VIBROIMPACT AT A SEISMIC JOINT BETWEEN ADJACENT STRUCTURES

Richard K. Miller[I]

SUMMARY

An exact solution is presented for the steady single-impact-per-cycle oscillations of adjacent undamped single story frames separated by a gap and subjected to harmonic base motion. The impacts are assumed to be inelastic with coefficient of restitution $0 \leq e \leq 1$. Parameter studies are presented which illustrate the effects of changes in the excitation frequency and amplitude, coefficient of restitution, and gap size. It is shown that in some cases inelastic vibroimpact can actually protect both frames from excessive stress resultants due to resonance.

INTRODUCTION

Large structures are often constructed with seismic joints or narrow gaps between adjacent but independent substructures. Examples include multistory office and parking structures, multispan bridges, and mechanical equipment within nuclear power plants. The gap size is intended to be large enough to prevent collision between substructures during earthquakes, but such collisions have occured in past earthquakes [1] with resulting structural damage. Estimating the effects of such collisions can be important, as for example in determining the extent of necessary upgrading of a nuclear power plant for increased seismic requirements.

While procedures for the analysis of vibroimpact are well known [2], the vibroimpact of adjacent structures during earthquakes has only recently been studied [3,4]. Presented in this paper is an analysis of the steady single-impact-per-cycle motion at a seismic joint between adjacent structures using the simplified classical notion of a constant coefficient of restitution to account for energy dissipation during impact. The results indicate that a properly designed seismic joint may actually help protect both structures from excessive stress resultants during earthquakes.

FORMULATION

Consider the two adjacent undamped single-story frames separated by a seismic gap of width d, as shown in Fig. 1. Let $\bar{y}_1$ and $\bar{y}_2$ denote the lateral displacements of the left frame and right frame, respectively. Let m_i and k_i denote the effective mass and stiffness of the i-th frame ($i=1,2$). Furthermore, let the system be subjected to steady harmonic base motion with displacement amplitude z_0, circular frequency ω, and arbitrary phase α.

Let the separation between frames $\bar{x}$ be defined as

[I] Associate Professor, Department of Civil Engineering, University of Southern California, Los Angeles, California 90007

$$\bar{x} \equiv \bar{y}_2 - \bar{y}_1 \quad . \tag{1}$$

Then the non-dimensional equations of motion may be written as

$$\begin{aligned} \ddot{x} + x &= (\Omega - 1) y_1 \\ \ddot{y}_1 + \Omega y_1 &= \eta\delta\cos(\eta^{\frac{1}{2}}\tau + \alpha) \end{aligned} \tag{2}$$

so long as $x > -1$, where

$$\begin{aligned} x &= \bar{x}/d \quad ; \quad y_1 = \bar{y}_1/d \quad ; \quad y_2 = \bar{y}_2/d \\ \delta &= z_0/d \quad ; \quad \Omega = \omega_1^2/\omega_2^2 \quad ; \quad \eta = \omega^2/\omega_2^2 \\ \tau &= \omega_2 t \quad ; \quad \omega_1^2 = k_1/m_1 \quad ; \quad \omega_2^2 = k_2/m_2 \end{aligned} \tag{3}$$

and a dot denotes differentiation with respect to τ. However, when $x = -1$, an impact occurs between frames, and Eqs. 2 do not apply. For the purpose of this analysis, an impact will be assumed to consist of an instantaneous change in the velocity of each frame. Requiring these changes in velocity to conserve linear momentum, and allowing inelastic impact with coefficient of restitution e $(0 \le e \le 1)$, it can be shown that

$$\begin{aligned} \dot{x}^+ &= -e\dot{x}^- \\ \dot{y}_1^+ &= \dot{y}_1^- + \mu(1+e)\dot{x}^-/(1+\mu) \end{aligned} \tag{4}$$

where the minus and plus denote velocities immediately before and after impact, respectively, and where the mass ratio μ is defined as

$$\mu = m_2/m_1 \tag{5}$$

SINGLE-IMPACT-PER-CYCLE OSCILLATION

Solutions of Eqs. 2 which are periodic with same period as the harmonic base excitation, and which involve exactly one impact between frames during each period of oscillation are called single-impact-per-cycle oscillations. Such oscillations constitute the predominant type of steady motion observed in laboratory experiments with small scale models of the system shown in Fig. 1.

During such motion, the impact occurs at different absolute times τ within the cycle depending on the phase α of the excitation. Choosing α such that the impact occurs at $\tau = 0$, the general solutions of Eqs. 2 may be written as

$$x(\tau) = \left[-1 + y_1(0^+) - \frac{\eta\delta}{(1-\eta)}\cos\alpha\right]\cos\tau + \left[\dot{x}(0^+) + \dot{y}_1(0^+) + \frac{\eta^{3/2}\delta}{(1-\eta)}\sin\alpha\right]\sin\tau$$

$$-\left[y_1(0^+) + \frac{\eta\delta}{(\eta-\Omega)}\cos\alpha\right]\cos\Omega^{\frac{1}{2}}\tau - \frac{1}{\Omega^{\frac{1}{2}}}\left[\dot{y}_1(0^+) - \frac{\eta^{3/2}\delta}{(\eta-\Omega)}\sin\alpha\right]\sin\Omega^{\frac{1}{2}}\tau$$

$$- \frac{(\Omega-1)}{(1-\eta)}\frac{\eta\delta}{(\eta-\Omega)}\cos(\eta^{\frac{1}{2}}\tau + \alpha) \qquad (6)$$

$$y_1(\tau) = \left[y_1(0^+) + \frac{\eta\delta}{(\eta-\Omega)}\cos\alpha\right]\cos\Omega^{\frac{1}{2}}\tau + \frac{1}{\Omega^{\frac{1}{2}}}\left[\dot{y}_1(0^+) - \frac{\eta^{3/2}\delta}{(\eta-\Omega)}\sin\alpha\right]\sin\Omega^{\frac{1}{2}}\tau$$

$$- \frac{\eta\delta}{(\eta-\Omega)}\cos(\eta^{\frac{1}{2}}\tau + \alpha) \qquad (7)$$

The range of τ over which solutions in Eqs. 6 and 7 apply is from 0^+ to P^-, where

$$P = 2\pi/\eta^{\frac{1}{2}} \qquad (8)$$

is the value of τ corresponding to one period of the excitation. In order for periodic motion to occur, another impact must occur at $\tau=P$, and the solution must repeat itself during the next cycle of oscillation. Thus, the values of the solution at $\tau=0^+$ and at $\tau=P^-$ must be related by the impact conditions given in Eqs. 4. In particular, these periodicity conditions require

$$\begin{aligned} x(P^-) &= -1 \quad ; \quad \dot{x}(P^-) = -\dot{x}(0^+)/e \\ y_1(P^-) &= y_1(0^+) \; ; \quad \dot{y}_1(P^-) = \dot{y}_1(0^+) + \frac{\mu(1+e)}{e(1+\mu)}\dot{x}(0^+) \end{aligned} \qquad (9)$$

Evaluating Eqs. 6 and 7 and their derivatives at $\tau=P$ and enforcing the four conditions in Eqs. 9 results in nonlinear algebraic equations in the four unknowns $x(0^+)$, $y_1(0^+)$, $y_2(0^+)$, and α. Solving these simultaneous equations, it can be shown that

$$\alpha = \tan^{-1}\left[\frac{BC \pm A(A^2+B^2-C^2)^{\frac{1}{2}}}{AC \mp B(A^2+B^2-C^2)^{\frac{1}{2}}}\right] \qquad (10)$$

where two solutions for α are possible, one corresponding to the upper signs and one to the lower signs in Eq. 10, and where

$$A = c_1/a_1 - c_2/a_2 \quad ; \quad B = d_1/a_1 - d_2/a_2 \quad ; \quad C = b_2/a_2 - b_1/a_1$$

$$a_1 = \sin P - \frac{(1+e)\mu}{2e(1+\mu)}\left[\frac{\Omega^{\frac{1}{2}}\sin P(1-\cos\theta) - \sin\theta(1-\cos P)}{\Omega^{\frac{1}{2}}(1-\cos\theta)}\right]$$

$$a_2 = \left(\frac{1}{e} + \cos P\right) - \frac{(1+e)\mu}{2e(1+\mu)}\left[\frac{\Omega^{\frac{1}{2}}(1+\cos P)(1-\cos\theta) - \sin\theta\sin P}{\Omega^{\frac{1}{2}}(1-\cos\theta)}\right]$$

$$b_1 = (1 - \cos P) \quad ; \quad b_2 = -\sin P$$

$$c_1 = \eta\delta\,\frac{(1-\cos P)(\Omega-1)}{(1-\eta)(\eta-\Omega)} \quad ; \quad c_2 = \eta\delta\,\frac{\sin P(\Omega-1)}{(1-\eta)(\eta-\Omega)}$$

$$d_1 = \eta^{\frac{1}{2}}c_2 \quad ; \quad d_2 = -\eta^{\frac{1}{2}}c_1 \quad ; \quad \theta = \Omega^{\frac{1}{2}}P \tag{11}$$

After having obtained α, the remaining three unknowns may be obtained from the expressions

$$\dot{x}(0^+) = (b_1 + c_1\cos\alpha + d_1\sin\alpha)/a_1$$

$$\dot{y}_1(0^+) = -\frac{(1+e)\mu}{2e(1+\mu)}\,\dot{x}(0^+) + \frac{\eta^{3/2}\delta\sin\alpha}{(\eta-\Omega)} \tag{12}$$

$$y_1(0^+) = -\frac{(1+e)\mu}{2e(1+\mu)}\,\frac{\sin\theta}{\Omega^{\frac{1}{2}}(1-\cos\theta)}\,\dot{x}(0^+) - \frac{\eta\delta\cos\alpha}{(\eta-\Omega)}$$

Solutions for $x(\tau)$ and $y_1(\tau)$ may now be constructed by inserting the values for α, $\dot{x}(0^+)$, $\dot{y}_1(0^+)$, $y_1(0^+)$ from Eqs. 10 and 12 into Eqs. 6 and 7. However, only those solutions which satisfy the additional constraint that $x > -1$ for $0 < \tau < P$ represent physically realizable motion, since $x < -1$ would require penetration of one frame by the other.

NUMERICAL RESULTS

Shown in Figs. 2, 3 and 4 are plots of the maximum absolute value of periodic displacements x, y_1, and y_2, respectively, as functions of the excitation frequency parameter, η. These maximum displacements provide an indication of the magnitude of the overall stress resultants developed within the impacting frames. The lines in these figures represent physically realizable solutions to the equations for single-impact-per-cycle motion for three different levels of the excitation amplitude parameter δ. (Before further discussion, it should be noted that some physically realizable solutions for single-impact-per-cycle motion have been omitted from the figures. These omitted solutions exist only over very small frequency bands in the range $0 < \eta < 1$, and apparently begin with smallest frequency 1/2, 1/4, etc.) Furthermore, Figs. 2, 3 and 4 correspond to the case of perfectly elastic impact ($e=1$) between frames with identical mass ($\mu=1$) but with a two-fold difference in stiffness ($\Omega=2$). Thus, when separated from each other by great distance, frame 1 achieves resonance when $\eta=2$ and frame 2 achieves resonance when $\eta=1$, in this case.

Several interesting features of the response are displayed in Figs. 2, 3 and 4. Note from Eqs. 1 and 3, and from Fig. 1 that when $|x|_{max} < 1$, no impact occurs, and the response of the frames is simply the sinusoidal response of two independent linear systems. Thus, the response curves in Fig. 2 for $|x|_{max} < 1$ are determined from a linear analysis, and a discontinuity in slope of the response curves is observed when impact first occurs at $|x|_{max} = 1$. The response for $|x|_{max} > 1$ is nonlinear, and corresponds to single-impact-per-cycle vibroimpact. These nonlinear response curves are qualitatively similar in behavior to the nonlinear vibration of a two-mode dynamical system with hardening spring characteristics. For such an analogous nonlinear system, the effective natural frequencies

increase with increasing amplitude of response, and sudden jumps in the response amplitude are observed for small changes in the excitation frequency in some regions. From Fig. 2 it appears in this vibroimpact case that the effective natural frequency in the first mode is less than 2 for all amplitudes of response, but that the effective natural frequency in the second mode may continually increase as the response amplitude increases. Since the system in Fig. 2 is conservative, response amplitudes may become unbounded at some finite frequency between 1 and 2, and thus nonlinear resonance is possible. Of course, nonlinear resonance would not occur in real structures since it is well known [5] that the coefficient of restitution is reduced significantly at large impact velocities. Also shown in Fig. 2 is the effect of increasing the amplitude of base excitation, z_0, or of decreasing the gap size, d, either of which results in an increase in the excitation amplitude parameter, δ. Note that the response amplitude at a given frequency is always increased by increasing δ. Note also that when $\delta=1$ and for $\eta\cong 0.6$-0.65, single-impact-per-cycle motion is not possible. If, in fact, steady periodic motion exists in this range of frequencies, it must take the form of more complicated multiple impact-per-cycle or multiple-cycle-per-impact oscillations, neither of which are considered herein.

The general features of the response just described may also be observed in Figs. 3 and 4. However, the qualitative behavior of the response curves for y_1 and y_2 is more complex because these curves display the transition from one-mode linear response to two-mode nonlinear response, whereas the curves for x involve two modes in both the linear and nonlinear response regions.

Shown in Figs. 5, 6 and 7 are the response curves for the same system except that the collisions here are considered to be slightly inelastic, with coefficient of restitution e=0.8. The main effect of the inelastic collisions is to absorb a percentage of the kinetic energy in the system during each cycle, and thus to provide a form of damping. As a result, comparing response curves in Figs. 5, 6 and 7 with those in Figs. 2, 3 and 4, it is seen that the effective damping of the inelastic collisions is sufficient to "close" the upward branches of the response curves and prevent unbounded response, at least in the second mode. The inelasticity of collisions in the first mode for $\delta=0.1$ apparently disrupts the pattern of motion sufficiently to extinguish single-impact-per-cycle motion for frequencies larger than about $\eta\cong 1.48$. A similar disruption of nonlinear resonance may occur at larger amplitudes for $\delta=0.5$ and $\delta=1.0$. Furthermore, the nonlinear response at any given frequency is generally reduced in amplitude by the energy dissipation during collisions.

Shown in Figs. 8, 9 and 10 are the response curves for the same system, but for highly inelastic collisions with coefficient of restitution e=0.2. Comparing Figs. 8, 9 and 10 with Figs. 5, 6 and 7, it is seen that the amplitude of nonlinear response is further reduced by the increase in energy dissipation during collisions. In fact, it is seen in the figures that the upward branches of the response curves are closed even in the first mode for $\delta=0.1$ and $\delta=0.5$, and that single-impact-per-cycle motion is extinguished in the first mode for $\delta=1.0$. Furthermore, the figures show that for e=0.2, vibroimpact between frames actually provides an efficient mechanism for preventing resonance and limiting magnification of overall stress resultants in each frame, and therefore may be beneficial. For

systems with fixed gap size d, the figures indicate that the degree of protection depends on the amplitude of excitation, z_0, being greatest for small z_0. For many structural materials, the effective coefficient of restitution may be expected to be as low as 0.2 only for relatively large impact velocities [5]. In order to reduce e as much as possible for small impact velocities, it may be necessary to place some energy absorbing material in the gap between frames in order to protect adjacent frames from impact damage during sustained ground motion.

ACKNOWLEDGMENTS

Portions of this investigation were funded by the National Science Foundation under Grant No. PFR-7701096, and by the Regents of the University of California, while the author was a member of the faculty at the Santa Barbara campus.

REFERENCES

[1] Miller, R.K., and Felszeghy, S.F. (1978). "Engineering Features of the Santa Barbara Earthquake of August 13, 1978," Report No. UCSB-ME-78-2, Earthquake Eng. Res. Inst., Berkeley, California, pp. 11.1-11.6.

[2] Kobrinskii, A.E. (1969). Dynamics of Mechanisms with Elastic Connections and Impact Systems, ILIFFE Books Ltd., London.

[3] Shizuo, S. (1974). "Earthquake Caused Collision of Adjacent Buildings" Japan Arch. Soc. Trans., Vol. 221, pp. 1-7 (in Japanese).

[4] Wolf, J.P., and Skrikerud, P.E. (1979). "Mutual Pounding of Adjacent Structures During Earthquakes," Trans. 5th Int. Conf. on Struc. Mech. in Reactor Tech., Berlin, Paper K8/9.

[5] Goldsmith, W. (1960). Impact, The Theory and Physical Behavior of Colliding Solids, Edward Arnold Ltd., London, pp. 257-262.

FIGURES

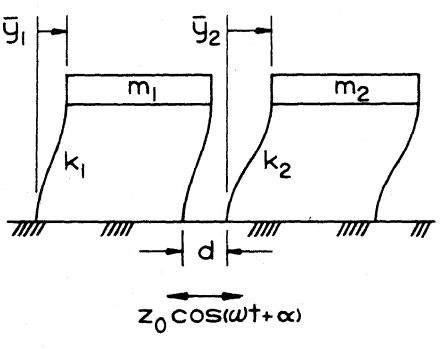

Fig. 1: Adjacent Frames with Harmonic Base Excitation

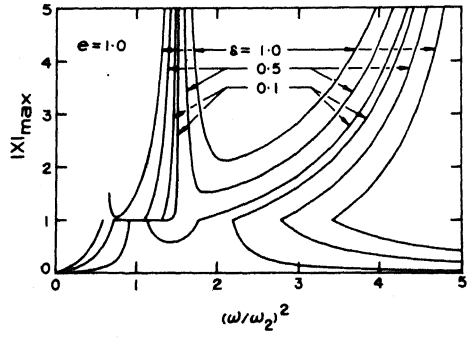

Fig. 2: Maximum Response x vs. η for System with $\mu = 1$, $\Omega = 2$, and $e = 1$

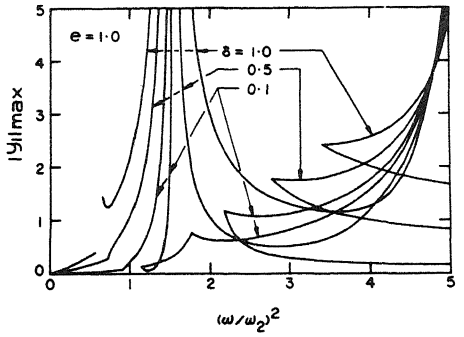

Fig. 3: Maximum Response y_1 vs. η for System with $\mu = 1$, $\Omega = 2$, and $e = 1$

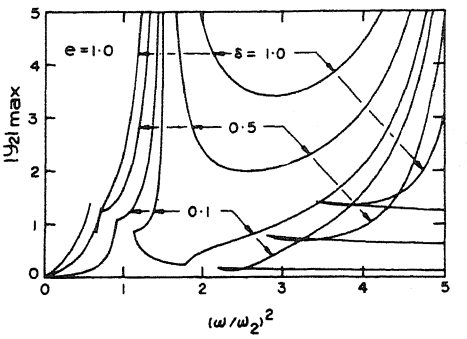

Fig. 4: Maximum Response y_2 vs.η for System with $\mu = 1$, $\Omega = 2$, and $e = 1$

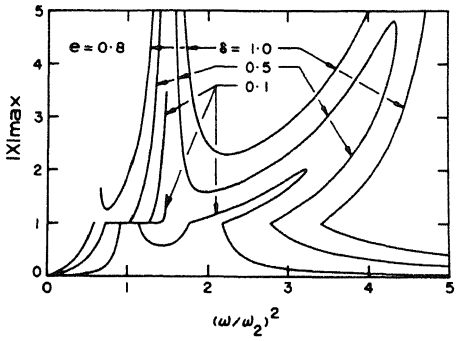

Fig. 5: Maximum Response x vs. η for System with $\mu = 1$, $\Omega = 2$, and $e = 0.8$

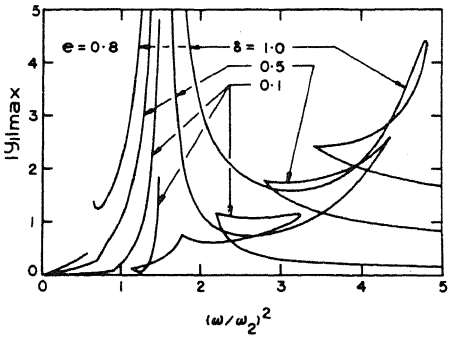

Fig. 6: Maximum response y_1 vs. η for System with $\mu = 1$, $\Omega = 2$, and $e = 0.8$

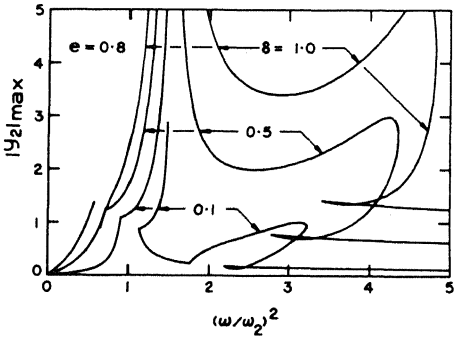

Fig. 7: Maximum Response y_2 vs. η for System with $\mu = 1$, $\Omega = 2$, $e = 0.8$

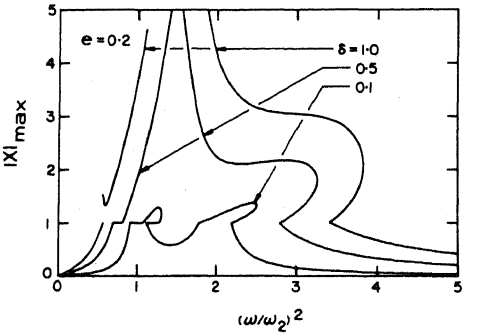

Fig. 8: Maximum Response x vs. η for System with $\mu = 1$, $\Omega = 2$, and $e = 0.2$

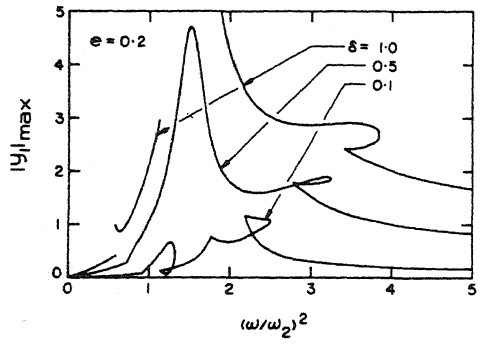

Fig. 9: Maximum Response y_1 vs. η for System with $\mu = 1$, $\Omega = 2$, and $e = 0.2$

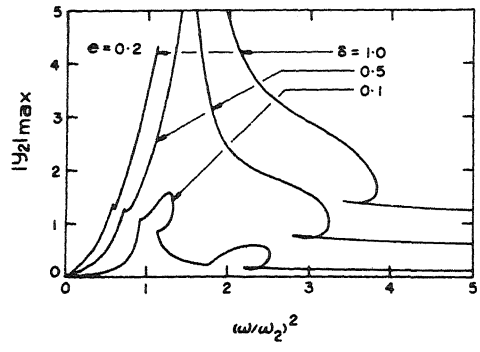

Fig. 10: Maximum Response y_2 vs. η for System with $\mu = 1$, $\Omega = 2$, and $e = 0.2$